



Title	A fractographic analysis of delamination within multidirectional carbon/epoxy laminates
Authors(s)	Gilchrist, M. D., Svensson, N.
Publication date	1995-01
Publication information	Gilchrist, M. D., and N. Svensson. "A Fractographic Analysis of Delamination within Multidirectional Carbon/Epoxy Laminates." Elsevier, January 1995. https://doi.org/10.1016/0266-3538(95)00099-2 .
Publisher	Elsevier
Item record/more information	http://hdl.handle.net/10197/5919
Publisher's statement	This is the author's version of a work that was accepted for publication in Composites Science and Technology. Changes resulting from the publishing process, such as peer review, editing, corrections, structural formatting, and other quality control mechanisms may not be reflected in this document. Changes may have been made to this work since it was submitted for publication. A definitive version was subsequently published in Composites Science and Technology (55, 2, (1995)) DOI: http://dx.doi.org/10.1016/0266-3538(95)00099-2
Publisher's version (DOI)	10.1016/0266-3538(95)00099-2

Downloaded 2026-05-02 00:27:53

The UCD community has made this article openly available. Please share how this access benefits you. Your story matters! (@ucd_oa)



© Some rights reserved. For more information

A FRACTOGRAPHIC ANALYSIS OF DELAMINATION WITHIN MULTIDIRECTIONAL CARBON/EPOXY LAMINATES

M. D. Gilchrist^a & N. Svensson^b

^a*Mechanical Engineering Department, University College Dublin, Belfield, Dublin 4, Republic of Ireland*

^b*Swedish Institute for Fibre and Polymer Research, Box 104, S-431 22 Mölndal, Sweden*

Abstract

Multidirectional laminates of the continuously reinforced carbon/epoxy composite T300H/914C have been tested under static and fatigue conditions by the use of fracture mechanics coupons. Loadings of pure mode I, pure mode II and different ratios of mixed mode I/II, i.e. opening tension and sliding shear, have been applied to double cantilever beam (DCB), end-loaded split (ELS), fixed-ratio mixed-mode (FRMM), and mixed-mode bending (MMB) specimens.

Optical and scanning electron microscopy techniques were used to identify distinguishing fractographic features and to establish the differences between static and fatigue fracture, as well as the differences between the various modes of fracture. The cusp angle and the amount of fibre pull-out on the fracture surface can be used to characterise the different loading modes. A large amount of fibre pull-out is the dominant feature of a mode I fracture whereas cusps are characteristic features of a mode II fracture.

Fatigue fracture surfaces exhibited slightly more debris than static fracture surfaces: this is thought to be due to the fretting nature of fatigue. For the same reason, shear cusps (hackles) were more rounded and less distinct in fatigue than on static fracture surfaces. In certain fatigue cases, it was observed that polyethersulphone (PES), a toughening agent used in the formulation of the epoxy resin, came out of the matrix; the reason for this is not fully understood.

Keywords: fractography, T300/914, carbon/epoxy composites, multidirectional laminates, fracture, delamination

1 INTRODUCTION

As the structural applications for fibre-reinforced polymeric composites continue to increase, so too does the need for a thorough understanding of the

fundamental failure processes in the different material systems. Much work has been done during the last two decades on the fractography of composites but more is needed if a fundamental understanding and a database¹ of the mechanisms and characteristics of fracture for different composite systems are to be established.

Delamination is one of the most common reasons for failure of composite laminates (e.g. from bending, interlaminar shear or impact) and can cause major reductions in the stiffness or strength of a structure. Delaminations grow between laminae as a consequence of the presence of fibres above and below a ply interface.² However, delaminations can be relatively difficult to detect and quantify since they constitute sub-surface damage. The present paper concentrates on the fractographic characteristics of delamination in multidirectional laminates under different known loading modes. These known modes of loading have been applied by using standard fracture mechanics testing methods. Specifically, these included double cantilever beam (DCB),³ end-loaded split (ELS),⁴ fixed-ratio mixed-mode (FRMM)⁴ and mixed-mode bending (MMB)⁵ test coupons under both static and fatigue loading conditions. The material examined was T300/914, a carbon-fibre/epoxy composite supplied by Ciba-Geigy Composites in unidirectional prepreg form. From this, a $[(- 45^{\circ}/0^{\circ}/ + 45^{\circ})_{2s}]_{\text{anti}}$ laminate sheet was laid up where the subscript 'anti' denotes an antisymmetric laminate. The complete stacking sequence was therefore:

$$\begin{aligned} & -45^{\circ}/0^{\circ}/45^{\circ}/-45^{\circ}/0^{\circ}/45^{\circ}/45^{\circ}/0^{\circ}/-45^{\circ}/45^{\circ}/0^{\circ}/-45^{\circ}/ \\ & 45^{\circ}/0^{\circ}/-45^{\circ}/45^{\circ}/0^{\circ}/-45^{\circ}/-45^{\circ}/0^{\circ}/45^{\circ}/-45^{\circ}/0^{\circ}/45^{\circ} \end{aligned}$$

Artificial starter delaminations along the $+45^{\circ}/-45^{\circ}$ interface, i.e. the midplane, were created by using non-adhesive PTFE film inserts of $13 \mu\text{m}$ thickness.

Delamination in composite structures is usually

associated with fracture along an interface where the adjacent plies are of different orientation, i.e. in multidirectional laminates, whereas delamination in fracture toughness specimens is common to unidirectional laminates. Despite some difficulties associated with fibre bridging and R-curve effects, it is relatively easy to quantify the fracture energy associated with delamination in unidirectional laminates since the damage is effectively constrained along a $0^\circ/0^\circ$ interface by the fibres within the plies abutting the interface. Quantifying the toughness associated with delamination along a particular interface in multidirectional laminates is complicated by the fact that the damage often propagates towards and along other interfaces: the damage in such instances can also consist of fracture mechanisms other than delamination. However, the toughness associated with delamination along a multidirectional interface can be far greater than that of a unidirectional interface. This can be quantified by using non-adhesive inserts to simulate a starter crack and edge delaminations in fracture mechanics coupons, as has been done in the present work. The artificial edge delaminations help to ensure that the delamination growth remains along the particular multidirectional interface.

The different fracture mechanisms in mode I and II result in very different values of G_{Ic} and G_{IIc} for brittle resins.⁶ For very ductile resins the ratio of G_{IIc}/G_{Ic} is very close to 1.0 as the fracture processes in mode I and II are similar.⁷ Above a certain threshold ($\sim 250 \text{ J/m}^2$) less than a third of the improved resin toughness is transferred to the composite while resins with lower toughnesses usually show a composite toughness twice or three times that of the plain resin.⁸

A significant matrix feature is cusps which also have been referred to as hackles, lacerations, scallops, platelets, shingles, a stacked lamellar structure and serrations. Purslow⁹ recognised the need to develop a general terminology and the term 'cusps' will be used throughout this article. The cusps are oriented perpendicular to the fibres, bent over along them with a width approximately equal to the distance between the fibres. They are usually found in the resin-rich regions where the fibre separation is more than one fibre diameter. The slope of the cusps is the same all over one surface and opposite on the mating surface¹⁰ even if the delamination changes plies during propagation.¹¹ Different theories for the formation of cusps have been proposed. It is now generally accepted that the matrix in the interlaminar region ahead of a crack tip will fracture in a brittle manner because of the resolved stresses to which it is subjected.¹² When a mode II component of load is present, crack propagation in a brittle matrix occurs by the coalescence of sigmoidally-shaped microcracks. This phenomenon has been observed by means of *in situ* SEM by a number of workers.^{6,7} The coalescence

occurs near the fibre/resin interface at the upper or lower boundary of the resin-rich interlaminar region. When coalescence has started at one ply interface it will continue there as the stress redistribution involved will favour a continued coalescence at the same interface.⁷ Other workers have reported cusps on both fracture surfaces as the crack propagation alternates from one side of the interlaminar region to the other.^{13,14} The tilt of the cusp can either be in the direction of crack propagation or in the opposite direction. Therefore, cusps alone cannot be used to determine the direction of crack propagation. Opposing cusps on the other mating surface are depressed concave areas and are referred to as scallops.

In pure mode II loading the cracks that cause cusps would, according to theory, form at an angle of 45° to the fracture plane. This angle would then decrease due to an increasing component of mode I loading and for pure mode I no cusps would form.¹³ Experimental evidence only supports this qualitatively.^{13,15,16} Cusp angles, significantly greater than 45° , have been observed and explained⁷ as attaining a more inclined position because of rotation due to shear loading just prior to the microcrack coalescence. This rotation would position the microcrack more vertically and open up the microcrack near the boundary where the coalescence takes place. The tip of the cusp has been observed to be bent over in the direction of relative motion of the adjacent plies.¹³ River markings and microflow can be found on both scallops and cusps^{13,17} and these give an indication of the crack propagation involved in the formation of features.¹⁸ These rivers may also be used to determine the overall crack propagation direction.⁷ The rivers are seen to grow out from the fibre/matrix interface and into the cusp. At higher crack velocities the cusps are smaller due to a smaller damage zone around the crack tip.¹⁹ Closer fibres will give shorter cusp spacing as more microcracks are needed in the resin to accommodate a given strain.¹¹ Cusps are only found in relatively brittle systems as they are formed from microcrack nucleation ahead of the crack tip.⁷ Due to the higher ductility of tougher resins, which have a lower ratio of G_{IIc}/G_{Ic} ,²⁰ fewer cusps are apparent in tough resins than in brittle resins. Cusps in mode III loading have also been observed.^{21,22}

Fibre pull-out is an important fracture surface characteristic. Russell and Street²⁰ identified that the amount of fibre pull-out is greater in fatigue than in static loading. Friedrich¹⁹ observed that the amount of pull-out was greater in PEEK than in epoxy-matrix systems. The amount of pull-out was greater in mode I than in mode II for the epoxy system whilst more fibre ends were found on the mode II fracture surface in the PEEK system. No difference in the density of broken fibres per unit area of fracture surface could

be found at different crack propagation velocities. However, Hahn and Johannesson²³ did not establish any relationship between the loading mode and the amount of fibre fracture.

The fibres ahead of the main crack can be considered as high modulus inclusions in a low modulus matrix subjected to a tensile stress normal to the plane (assuming mode I loading). The associated stress distribution around a fibre indicates that failure will take place at the highly stressed regions at the top and bottom of the fibre. Where the radial stress changes from tensile to compressive, local shear yielding will be induced in the matrix. Matrix failure will occur at the sides of the fibres leaving flanges of resin on the fibres as they are peeled out.²⁴ Fibre fractures in pure mode II do not originate in the same way as in loads with a mode I component (i.e. from fibres bending). In such cases the fibres which cross the shear plane will fracture in tension or compression. All fibres that fail in tension will have their fibre ends in one direction and those failing in compression in the opposite direction.²⁵

Cyclic loading causes fretting and abrasion of the fracture surfaces which obscures most of the features.^{10,19,20} The wear down of cusps increases with the number of loading cycles but it is not possible to determine the fatigue life from the cusp morphology.¹¹ The macroscopic fracture surface is characteristically very flat.²⁶ Large amounts of resin debris is also a characteristic of fatigue failure. The damage zone around a crack tip is significantly larger in fatigue than in static loading.²⁷ Under a certain threshold strain energy release rate, G_{th} , no fatigue crack growth is observed.²⁸

Fatigue striations are frequently found in metals where their formation and significance are well understood. However, this is not the case for composites. Franz²⁹ studied the fatigue behaviour of plain epoxy resin and glass-fibre-reinforced epoxy (brittle). In the unreinforced epoxy, striation markings were found oriented perpendicular to the crack propagation direction with one striation corresponding to one load cycle. No striations were expected in the composites²⁹ as the matrix only sustained small stresses before failure in most epoxy composites (i.e. the fibres carry almost all of the load). For high strain to failure epoxies, however, fatigue striations could not be excluded. Some striations were found on small parts of delaminated surfaces and in fibre imprints. In the composites, the striations generally stepped out of plane while in the plain epoxy they stayed in-plane. The striations found in fibre imprints showed a great similarity with those in the plain epoxy. It was also observed that the spacing between the striations may vary and that striations may be oriented locally in a direction different to the global crack propagation direction.

Morris and Hetter³⁰ compared the fatigue fracture surface of multidirectional AS/3501-6 with that of a statically peeled-off surface ply. The main difference between the two surfaces was found to be fatigue striations. These were observed on fibres perpendicular to the fibre direction and in the epoxy matrix parallel to the fibres. More striations were present in the epoxy than on the fibres and these were also spaced closer together. A relationship between the number of striations and the number of fatigue cycles could not be established. The experiments indicated that no fatigue striations formed at a fatigue load greater than 70% of the ultimate tensile strength.

Mode II fatigue ($R = -1$) was studied for four different composites by Carlsson *et al.*¹⁰ where no fatigue striations were observed in either of the materials. Matrix debris was the dominant feature in the epoxy resins but some distorted cusps were also found. Six different composite systems, subjected to mode II fatigue, were examined by Hiley and Curtis.²⁸ Single phase thermoset resins could be ranked according to their toughness only by comparing the complexity of the fracture surfaces. Fatigue striations were observed but attempts to identify the forming mechanism and to relate the striation spacing to the number of loading cycles were unsuccessful. Matrix 'rollers' from the rolling of resin debris were observed. They were small close to the crack tip and their size increased away from the crack front. It is possible that these rollers decreased the friction between the surfaces during testing.

The fracture surfaces from edge delamination during tensile fatigue testing ($R = 0.1$ and $R = 0.5$) of AS4/3502 at two different stress levels were studied by Scrivner and Chan.³¹ For $\sigma = 0.85\sigma_{delam}$, where σ_{delam} is the stress at delamination onset, fibre/resin debonding was the primary failure mechanism and a few shallow cusps were seen. For $\sigma = 0.75\sigma_{delam}$ rows of larger cusps appeared along with the debonding. The cusp density was higher for $R = 0.1$; this is due to a more rapid coalescence of microcracks. The fractures had a mode I dominated appearance for both stress levels and this was confirmed by a finite element stress analysis.

T300 are PAN based carbon fibres with a diameter of about 7–8 μm manufactured by Torayca. They are surface treated with a thin (0.1–0.2 μm) epoxy polymer to improve resin adhesion and give a higher interlaminar shear strength.^{32,33} They are commonly used in prepregs with a variety of matrices. The Fibredux 914 resin, supplied by Ciba Composites, is widely used and Partridge³⁴ called it the standard high temperature epoxy system throughout Western Europe. It is a mixture of two glycidyl amine epoxy resins (MY 720 and ERL 0510) and a PES additive. The constituents are homogeneously mixed during manufacture and undergo a phase separation in the

curing process. The microstructure is a two phase structure containing a particulate phase and a connective phase. The continuous phase is very PES rich and the particles, or globules, are epoxy dominated.^{35,36} Bucknall and Partridge,³⁷ however, concluded that the nodules seen on the fracture surface were PES rich. They also observed that the fracture toughness and modulus were only marginally affected by different concentrations of hardeners and resins in spite of very different fracture morphologies. The matrix system can thus be regarded as a thermoplastic resin modified with epoxy particles where the presence of the epoxy particles reduces the toughness of the PES. It is therefore likely that the toughness would increase by lowering the amount of the epoxy phase. The size and distribution of the particles would also change by varying the formulation of the compound. Lowe³⁶ observed particles with a size of 0.8–1 μm ; irregular and bigger particles, up to 5 μm , were concluded to be clusters of the smaller particles. About 85% of the resin is in the particulate phase. A third phase can also be observed in composites as a thin coating surrounding the fibres. This phase is probably epoxy based. The thermoplastic is chiefly added to improve the processing characteristics by increasing the viscosity which will limit the formation of voids, control the dimensional stability and give a controlled resin flow during gelation and an easy fibre management.³⁴ The PES also reduces the chemical sensitivity of the resin and improves the toughness both in peel and shear. The microstructure has been seen to be sensitive to flaws and manufacturing conditions and microvoids are frequently present.³⁶ No difference in microstructure can be observed between the plain resin and the composite matrix phase.^{36,38} Fractography of composites using the 914 resin is complicated by the presence of the second phase and the morphology is not easily compared with that of single phase materials.^{9,28}

A fractographic examination³⁶ of a variety of typical fracture surfaces showed very little interfacial failures in unidirectional T300/914 carbon/epoxy laminates. The vast majority of the failures had occurred at the boundary between the coating matrix phase and the two-phase resin. This was concluded to be the weakest part of the composite. Plastic deformation was seen to increase with increased temperature but it was confined to the connective thermoplastic phase. Fracture never occurred through the particle phase and cracks tended to follow the interface between particles and the continuous matrix phase. As a result of this a few loose particles were seen on most of the fracture surfaces. The fracture mechanisms were independent of temperature; however, in mode I the two-phase resin pattern became more pronounced with increasing temperature. Cusps were identified in the shear-dominated mode II and intralaminar shear

failures. Very clean-cut fibre ends were seen as a sign of a strong fibre/matrix interface which allowed only little flexure of the fibres before fracture. A small amount of fibre pull-out is occasionally seen in mode I fracture.^{36,39} The fibre failure may occur from flaws on the fibre surface or from stress concentrations induced by the interphase region. Failure between the fibre and the interphase is very rare and occurs only in areas with a high volume fraction, v_f , of fibres. This kind of failure, however, increases with temperature in mode II.³⁶ No significant difference was detected by deCharentenay *et al.*⁴⁰ in the mode I surface morphology at moisture contents of 0.4 and 1.5%.

A clear distinction between static and fatigue mode II fracture surfaces of XAS/914 was reported by Corberand.²⁶ The static surface showed clean fibres, brittle matrix failure with nodules of PES embedded in the resin and cusp-like matrix features. In fatigue the nodules were free on the surface; this probably occurred from grinding of the surfaces. More nodules were seen at a higher number of fatigue cycles. The general appearance of the fracture surface was more flat than for the static surface. Loose nodules have also been observed by Henaff-Gardin and Lafarie-Frenot⁴¹ on the delamination surface in tensile fatigue testing of T300/914 cross-ply laminates. Occasional fatigue striations were seen by Hiley and Curtis²⁸ in mode II fatigue testing of XAS/914. These were oriented perpendicular to the fibre and direction of crack propagation.

A T300/914 fracture surface was examined by means of X-ray photoelectron spectroscopy (XPS) and scanning Auger microscopy (SAM) by Watts *et al.*³³ SAM showed a thin matrix layer on all fibres and this led to the conclusion that the fibre/matrix interface is strong. Carbon, nitrogen, oxygen, sulphur and silicon were found in XPS, the sulphur being from the PES additive and the silicon from a flow control agent.

2 EXPERIMENTAL

Fracture toughness specimens were subjected to a fractographic examination following testing in a variety of loading modes. The specimens were manufactured from 24-ply laminates with a stacking sequence of $(-45^\circ, 0^\circ, +45^\circ)_{2S}(+45^\circ, 0^\circ, -45^\circ)_{2S}$. As this is anti-symmetric the crack propagation was constrained to take place between a $+45^\circ$ and a -45° ply. An artificial delamination was simulated along the midplane by means of a non-adhesive 13 μm Kapton insert. The insert had edge delaminations along the length of the specimens to provide stable crack growth and to maintain the delamination propagating along the $+45^\circ/-45^\circ$ midplane interface. The fibre/resin system was T300/914 which consists of carbon fibres in a PES modified epoxy resin. The applied loading modes are given in Table 1 together with the

Table 1. The different fracture modes that have been examined in the present work and the respective methods used for fracture testing

Fracture mode	Coupon test method
Mode I (static)	DCB
Mixed mode I:II = 6:1 (static)	MMB
Mixed mode I:II = 4:3 (static)	ELS (asymmetric)
Mixed mode I:II = 3:4 (static)	MMB
Mixed mode I:II = 3:10 (static)	MMB
Mode II (static)	ELS
Mode I (fatigue)	DCB
Mixed mode I:II = 4:3 (fatigue)	ELS (asymmetric)
Mode II (fatigue)	ELS

particular test methods that were used. For the fatigue tests, a load ratio of $R = 0.1$ was used. The toughness specimens were broken, generally by hand, when the aluminium endblocks had been removed after testing in order to examine the opposing fracture surfaces.

The fracture surfaces of the specimens were examined in an optical microscope at quite low magnifications. The poor inherent spatial resolution of an optical microscope made it impossible to use high magnifications and a great deal of detail could not be obtained. Hence this technique was not very useful. Features that could be distinguished were resin-rich areas, regions with a large amount of fibre pull-out, the crack front and the change in fracture mode at the crack tip. However, most of these features could also be seen visually and consequently they are not discussed in detail here.

Samples of a size suitable for electron microscopy ($\sim 20 \text{ mm} \times 20 \text{ mm}$) were cut from the fractured specimens using a diamond-coated saw. Several samples were taken from both surfaces of each specimen. The areas considered to be most interesting were at the end of the insert (i.e. the start of the crack) and the area around the crack tip. Pressurised air was used to remove saw debris from the surface. Each sample was then mounted on an aluminium disc and its edges coated with conductive paint. The gold coating was carried out in an Edwards S150A sputter coater. Carbon coating did not provide as good a resolution as gold sputter coating. A JEOL JSM-5300 scanning electron microscope was used. For maximum resolution, Sawyer and Grubb⁴² recommend a high accelerating voltage, a small probe size, high beam current and long exposure times. These principles were followed but at magnifications above $3500\times$ the resolution and focus were in general unacceptable even though focus could sometimes be obtained at up to $7500\times$ depending on surface roughness, quality of coating, etc.

Micrographs of various features were taken from different regions of several samples of each fracture

specimen. Polaroid film was used for its ease of processing and development. The results of the SEM examination are presented for each mode in the following sections. In all micrographs, the arrow indicates the globally induced crack propagation direction, and the magnification and accelerating voltage are given.

3 RESULTS

3.1 Mode I

Mode I fracture surfaces are generally smooth with few fibre fractures.¹⁷ Ridges and valleys have been recognised as a characteristic of peel failures.⁴³ The matrix fracture is usually a clean cleavage type of fracture.¹² Some cusps were observed in AS1/3501-6 at elevated temperatures by Russell and Street,⁴⁴ but they did not observe any cusps in brittle epoxies.²⁰ Bascom *et al.*²⁴ found cusps in the areas between pulled-out fibres. These areas were bounded by featureless resin (AS4/3501-6) fracture which corresponded to catastrophic fast fracture. Cusp-like features found on mode I surfaces in multi-directional composites may be explained from shear stresses developing due to Poisson's contraction⁷ or the local presence of a shear stress.⁹ In other words, the local conditions at a crack-tip may not actually be pure opening tension or mode I. This may explain why rivers, valleys and cusps are sometimes found on what are predominantly peel surfaces. Small cusps have been observed in the grooves of pulled-out fibres.¹² These are formed by local shear stresses along the sides of the fibres during the pull-out process. According to Friedrich¹⁹ no distinction in surface morphology can be made between low and high crack opening velocities in carbon-fibre-reinforced epoxy (3501-6). Marom *et al.*⁴⁵ observed that under mode I loading of fabric-reinforced epoxy, the fracture surface morphology was not affected by the lamination angle.

Arcan *et al.*¹⁶ examined the fracture characteristics of a brittle (3501-6) and a toughened epoxy (F185) reinforced with unidirectional carbon fibres. Many clean fibres and fibre breaks were seen in the brittle matrix. Matrix failure mainly occurred close to the fibre/matrix interface. At the crack front the maximum tensile stress was normal to the fibres while ahead of the crack front shear stresses were present which resulted in cusps on the fracture surface. Between the fibres, smaller and denser cusps were seen due to a more complex state of stress. The fracture surface of the tougher resin had a rougher appearance with irregular cusps and fibres covered with resin. Regions of fast and slow crack growth could be distinguished. The former appeared whitish

with oriented fracture features while the latter were black and not oriented.

Smith and Grove,¹⁸ using a 3501-6 resin system, examined the effects of ply orientation ($0^\circ/0^\circ$, $0^\circ/90^\circ$ and $+45^\circ/-45^\circ$) at the delamination interface. Areas of cohesive resin failure were present at all interfaces with a larger amount for the cross-ply interfaces. No cusps were observed. River markings and microflow were found in these areas and were recognised as a characteristic of a mode I failure. The crack propagation direction could be determined from the convergent direction of the rivers. For the $+45^\circ/-45^\circ$ interface many rivers were found that did not correlate directly with the induced crack propagation direction but by averaging their propagation a coalescence with the main crack was obtained. The boundary between interlaminar peel and shear failure at a $0^\circ/90^\circ$ interface was seen to be serrated.⁴⁶ The serration was easily observed in an optical microscope and could be used to determine the direction of peel and the delamination sequence.

Hibbs and Bradley⁷ studied mode I crack propagation by means of *in situ* SEM in a brittle resin and three toughened resins. In the brittle resin the crack propagated by interfacial debonding. A limited amount of matrix microcracking was present behind the crack tip as was some occasional fibre bridging and pull-out. In the toughest resin, fracture occurred by resin deformation and occasional fibre/matrix debonding. Considerable deformation and microcracking was seen outside the resin-rich area between the plies.

In the present work on the T300/914 system, fibre pull-out was the dominant feature of the mode I fracture surface and this consisted mainly of fibre bundles rather than single fibres. The fibres were covered with a layer of resin indicating a strong interface (Fig. 1), whilst the resin itself was mainly featureless (Fig. 2). The extensive fibre pull-out shown

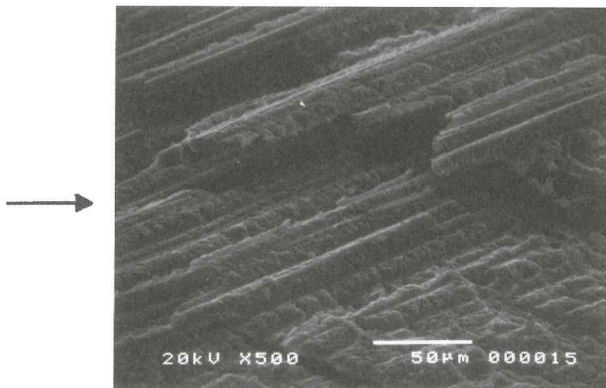


Fig. 1. Extensive fibre pull-out in mode I static fracture. The fibres are covered with resin. Cracks can be seen extending to the underlying ply (tilt angle is 70°). The globally induced direction of crack propagation is from left to right as shown by arrow.

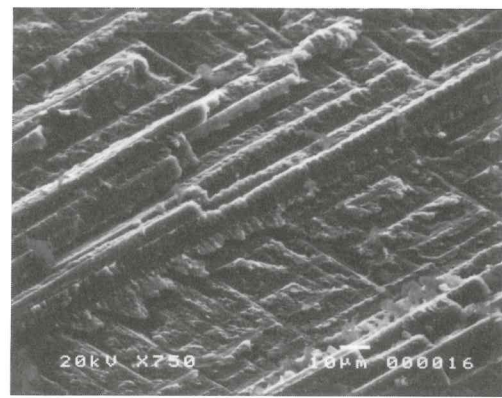


Fig. 2. Fibre pull-out with a lot of resin on the fibres and featureless resin fracture away from the fibres are characteristics for a mode I static failure (tilt angle is 75°). The globally induced direction of crack propagation is from right to left as shown by arrow.

in Fig. 1 is greater than that observed in unidirectional laminates; this degree of pull-out is peculiar to multidirectional laminates with delamination along a $+45^\circ/-45^\circ$ interface. The fracture energy associated with such a delamination is also greater than that of a $0^\circ/0^\circ$ interface. This higher fracture energy can be explained by considering the greater number of cracks that are generated in the laminate: cracks can be seen extending into the underlying plies in Figs 1 and 2.

The appearance of the mode I fatigue surfaces in the present work was very similar to the static mode I surface with the addition of resin debris and loose nodules. The surfaces of a single specimen prepared specifically to investigate the difference between fatigue and static fracture did not identify any significant differences between the static and the fatigue fracture surfaces. This specimen was opened statically in mode I after the last mode I fatigue cycle had been applied. Neither fatigue striations nor cusps were found on any mode I fatigue specimen.

3.2 Mode II

The mode II fracture surface for brittle epoxies is macroscopically flat with failure in the matrix and occasional fibre breaks. The fibres remain coated with a thin sheath of resin. Arcan *et al.*¹⁶ observed that cusps are more regularly spaced than in mode I and appear to be at an angle of 45° to the fracture plane whereas Smith and Grove¹⁸ noted that the cusps stand at an angle of $40-60^\circ$ to the fracture plane. Some fibre pull-out and many cusps have been identified in AS1/3501-6 laminates.⁴⁴ Donaldson¹² observed block-like cusps in the resin area between the fibres during pure shear loading. In tougher epoxies, clean fibres and regularly oriented cusps are seen which are also at an angle of 45° to the fracture plane. The initiation region, i.e. from the end of the insert to the beginning of a regular fracture surface, was seen to be about

10 μm in a brittle epoxy composite and 200 μm in an elastomer modified composite.¹⁶

During mode II loading of fabric-reinforced epoxy that is oriented at an angle to the crack propagation direction, the fracture mostly runs in the matrix and leaves shear kink bands perpendicular to the direction of crack growth.⁴⁵ In multi-directional lay-ups, where the shear occurs at an angle to the fibre direction of the adjacent plies, the cusps form at an angle to the fibres but perpendicular to the crack propagation direction.⁴⁷ An example of this was observed by Smith and Grove¹⁸ where the cusps at a $+45^\circ/-45^\circ$ interface were large and triangular but still oriented perpendicular to the induced crack. In failures along a $0^\circ/0^\circ$ ply interface cusps were seen on both fracture surfaces, while in cross-ply failures cusps could only be found on one of the surfaces.

In the present work, the macroscopic appearance of the mode II static fracture surface in T300/914 multidirectional laminates is flat with few fibre fractures being evident. Typical mode II static fracture surfaces can be seen in Figs 3 and 4 with rough resin fracture and some debris and nodules. The fibres are almost clean (Fig. 3) with only a thin sheath of resin around them. The cusps are more common, larger in size, more clearly defined and stand more upright than in any other mode. In Fig. 4 it looks as though there is a preference for the cusps to form at the fibres of the underlying ply. They also seem to be oriented perpendicular to the crack propagation direction. A short distance after the end of the insert, the crack jumped into a $0^\circ/45^\circ$ interface (not shown) and the surface appearance in this region is extremely flat and featureless indicating a much lower fracture energy. This implies that less energy has been required to generate the $0^\circ/45^\circ$ fracture surface.

The mode II fatigue fracture surfaces of this work consisted of large amounts of resin debris and loose

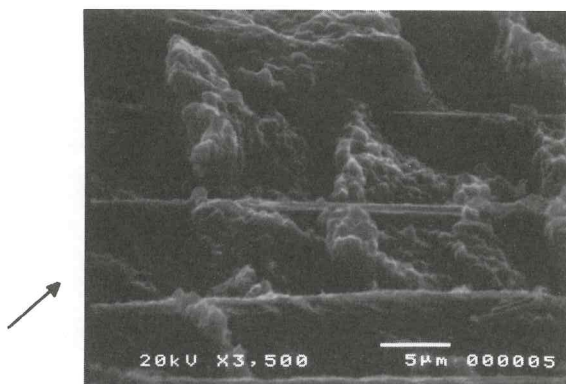


Fig. 3. Cusps standing at a large angle to the plane of a mode II static fracture surface. The cusps are present between the fibres (tilt angle is 75°). The globally induced direction of crack propagation is from bottom left to top right as shown by arrow.

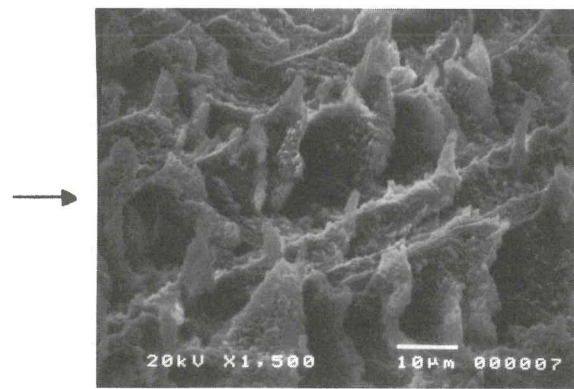


Fig. 4. Many upright cusps are visible and appear to stand on the underlying fibres on this mode II static fracture surface (tilt angle is 65°). The globally induced direction of crack propagation is from left to right as shown by arrow.

nodules in the resin between fibres. Small holes seemed to result from the extraction of the nodules. Significantly more broken fibres were observed than in static mode II fracture. The fibres are slightly cleaner than for statically failed mode II specimens. Cusps were present in relatively large quantities having about the same angle and appearance as for mode II static fracture. No fatigue striations could be observed on any mode II fatigue surface. The same phenomenon as in static mode II, i.e. the crack shifting plies, was also observed in mode II fatigue.

3.3 Mixed modes

As the component of mode II loading is increased, the general appearance of the mixed mode fracture surface gets rougher¹⁶ and also an increasing amount of more upright cusps is detected.⁷ At highly mode II dominated mixed modes, resin debris has been reported²³ and it is assumed that this originates from cusps that have been torn apart. Donaldson¹² investigated fracture surfaces from mixed mode loading. At a mixed mode ratio of 1:1 a large amount of cusps were seen. They were shallow, flat and regularly spaced. The fibre fractures on the surface were very clean as a result of the mode I component. In mixed mode I:II=0.27:1 the cusps were less regularly spaced and the fibre fracture showed characteristics of shear failure. Arcan *et al.*¹⁶ studied a mixed mode ratio of I:II=0.36:1 in brittle and toughened composites. A corrugated fracture surface was observed in the brittle resin with valleys and ridges along the fibre direction. Small, closely spaced cusps were seen between the fibres. These were thin, had a triangular shape and were curled at the tip. They stood up from the plane at an angle of about 40° . In the tough resin, deep longitudinal grooves and granular matrix failure in the form of random cusps were observed. Johannesson and Blikstad¹⁵ studied fracture surfaces of the same material subjected to

edge delamination. An increase in cusp angle with increasing mode III component was detected and for mode III dominated failures the cusp angles were close to 45° . This variation in cusp angle with mode mix has been used to explain the different G_c values observed.⁴⁸

The mixed mode I:II = 6:1 static fracture surfaces of the T300/914 multidirectional laminates of the present work were very similar to those observed in pure mode I loading. Less extensive pull-out and a rougher resin fracture appearance than that in pure mode I are the main differences, as shown in Fig. 5. Some few cusps were found due to the component of mode II loading. These cusps were quite shallow and not as well defined as in pure mode II.

The fracture surface of static mixed mode I:II = 4:3 is macroscopically flat. Occasional fibre pull-out is seen and the fibres have some resin on them and are not as clean as in pure mode II (Fig. 6). Very minute cusp-like features can be seen around the sites of pulled-out fibres. A fibre with resin flanges, or wings, is seen in Fig. 7. Ridge and valley formations are frequently found and they seem to form in the vicinity of the fibres of the underlying ply. Cusps are rare although in Fig. 8 they can be seen in a micrograph taken at a low tilt angle. Figure 9 shows cusps from the middle of the sample a few millimetres ahead of the insert. Resin debris and nodules are present due to mixed mode I:II = 4:3 fatigue fracture in relatively large amounts. Very little fibre fracture occurred. No clearly defined cusps were found but some shallow, worn cusps were seen. The fibres are cleaner of resin in the fatigue fracture compared to the static. No fatigue striations were found.

The global appearance of the mixed mode I:II = 3:4 static fracture surface was observed to be very flat and featureless with almost no fibre breaks being detected.

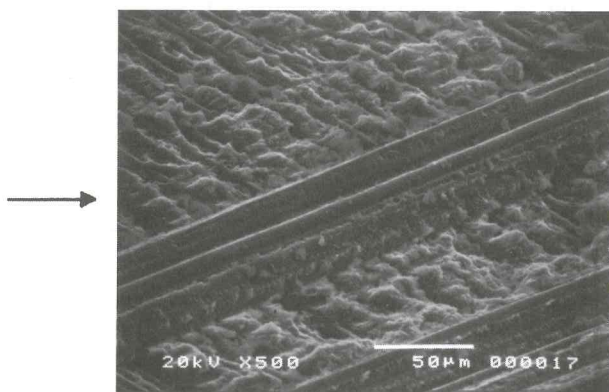


Fig. 5. The mixed mode I:II = 6:1 static fracture surface with featureless resin and fibre pull-out. The general appearance of this fracture surface is similar to that of a pure mode II surface, as shown in Fig. 2 (tilt angle is 65°). The globally induced direction of crack propagation is from left to right as shown by arrow.

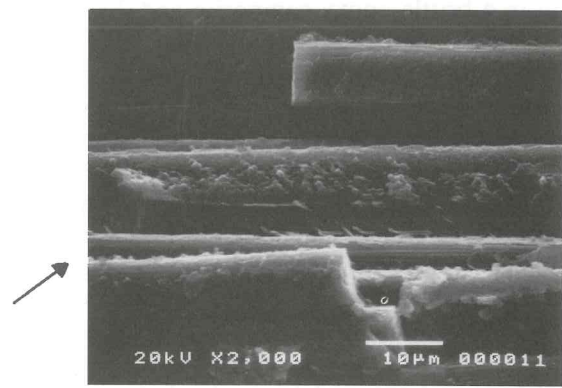


Fig. 6. Fractured fibres covered with a thin layer of resin. Minute cusps on a fibre are indicated by the arrow. Very sharp fibre fractures indicate good interfacial strength. Mixed mode I:II = 4:3 static fracture (tilt angle is 15°). The globally induced direction of crack propagation is from bottom left to top right as shown by arrow.

Some single fibres were seen on the surface rather than completely pulled-out fibre bundles. The fibres are covered with little resin. Cusps are relatively common but they are quite small and ill-defined, as shown in Figs 10 and 11.

The mixed mode I:II = 3:10 static fracture surface is also very flat macroscopically and extremely few fibre ends are found. Not surprisingly, the fibres are almost as clean as in pure mode II. The location of some ridges appears to be related to the sites of fibres on the opposite fracture surface. The very small amount of matrix found on the surface, especially between the fibres, implies that failure has taken place close to a ply interface. This would leave more resin on the other surface which is what has been observed. The cusps of Fig. 12 stand more upright than for the other mixed mode fracture surfaces which have been examined.

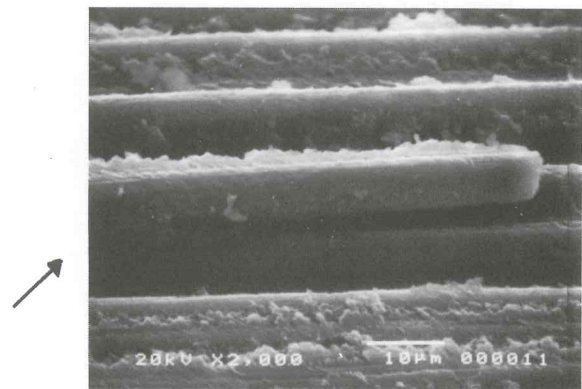


Fig. 7. A pulled-out fibre with resin flanges (similar to those cusps indicated in Fig. 6) found on a mixed mode I:II = 4:3 static fracture surface (tilt angle is 75°). The globally induced direction of crack propagation is from bottom left to top right as shown by arrow.

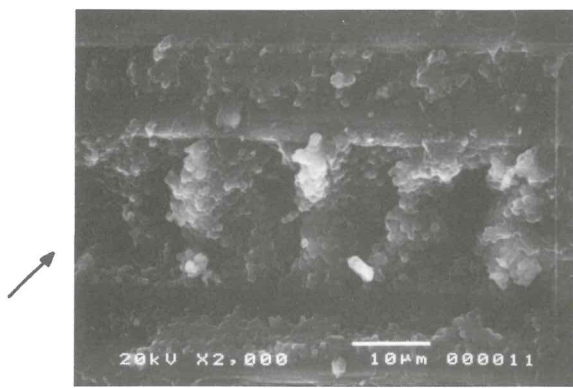


Fig. 8. Cusps as observed at a low tilt angle. A few resin nodules can be seen and the resin structure is quite clear. Mixed mode I:II = 4:3 static fracture (tilt angle is 15°). The globally induced direction of crack propagation is from bottom left to top right as shown by arrow.

3.4 The cusp angle

The cusp angle is quite difficult to determine accurately since the cusps in this particular resin system are not very clearly defined and hence it is hard to define the boundaries of the cusps. Another complicating factor is that the cusps do not show a great similarity with each other (see, for example, Figs 4 and 12), even in the same loading mode. The cusp angles for the different loading modes are given in Table 2. The errors in measuring cusp angle are estimated to be roughly $\pm 3^\circ$. Further studies relating cusp angle to the mode of fracture are to be discussed in future work.

3.5 Fibre pull-out

Another feature that is useful for characterising a fracture is the number of fibre ends present on the fracture surface. These result from the fibre pull-out process during fracture. The pull-out ought to increase with the mode I component and a relationship has

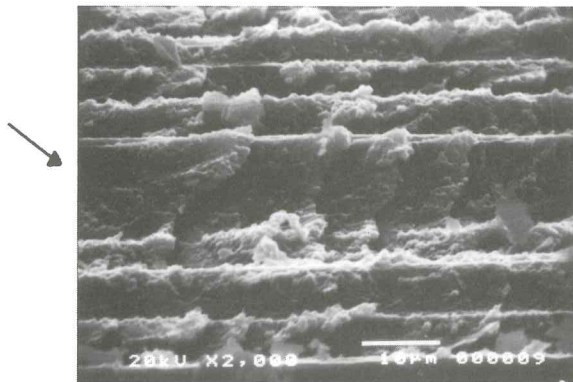


Fig. 9. Relatively well defined cusps from a mixed mode I:II = 4:3 static fracture. The cusps are present between the fibres (tilt angle is 70°). The globally induced direction of crack propagation is from top left to bottom right as shown by arrow.

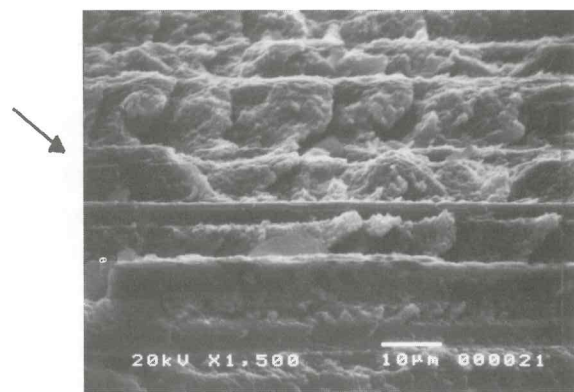


Fig. 10. Cusps on a mixed mode I:II = 3:4 static fracture surface. The cusps are present between the fibres (tilt angle is 70°). The globally induced direction of crack propagation is from top left to bottom right as shown by arrow.

tried to be established between loading mode and the number of fibre ends found on the fracture surface. A rapid increase in the number of broken fibres for static fractures as the component of mode I loading is increased was established, as shown in Table 3.

4 DISCUSSION

SEM fractography of T300/914 is difficult due to the two phase structure of the resin which effectively obscures most of the features described in previous fractographic work. Some constraints have also been imposed on the present work by the inability to obtain sufficient resolution at higher magnifications ($> 3500\times$) with the SEM that was used. In spite of these difficulties, most of the features reported by other workers have been detected. Of those not found, river markings are especially useful for establishing the direction of crack propagation in single phase resins.

The mode I fracture surface is best described by the general lack of cusps and by the large amount of fibre

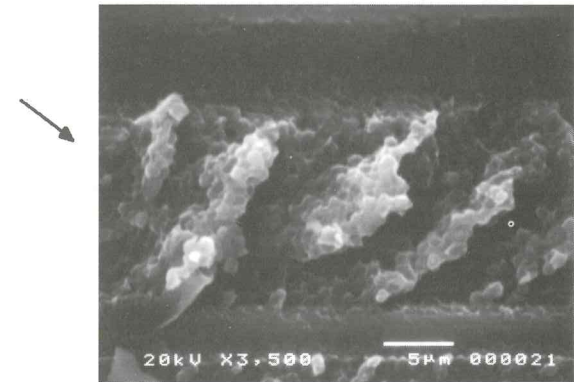


Fig. 11. Cusps oriented perpendicular to the fracture direction as observed at a low tilt angle. Mixed mode I:II = 3:4 static fracture (tilt angle is 10°). The globally induced direction of crack propagation is from top left to bottom right as shown by arrow.

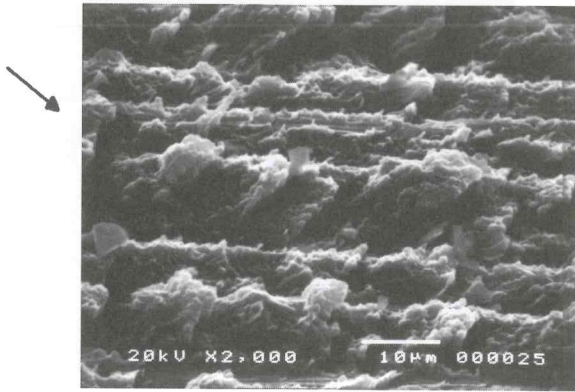


Fig. 12. Cusps which are oriented perpendicular to the crack direction and are standing more upright than on other mixed mode fracture surfaces. Mixed mode I:II = 3:10 static fracture (tilt angle is 65°). The globally induced direction of crack propagation is from top left to bottom right as shown by arrow.

ends present, see, for example, Figs 1 and 2, this latter point being in contradiction to Lowe³⁶ and Davies³⁹ who reported only occasional broken fibres in mode I. A reason for this may be the use of different lay-ups (unidirectional versus multidirectional), fracture mechanics specimens, precracks, inserts, etc. The pull-out is chiefly in bundles with the same amount of fibre pull-out on the opposing fracture surfaces. The fibre/matrix interface is very strong as the pulled-out fibres all have a resin layer on them and all the fibres have fractured very cleanly. This was also observed by Lowe.³⁶ Ridges and valleys, together with very little pull-out, mainly single fibres, and a general flat appearance are the characteristics of a mixed mode fracture surface having about equal mode I and II components. According to Purslow,⁹ ridges and valleys form under a combination of peel and shear stresses. The characteristics of a mode II fracture surface have been determined in the present work to be few broken fibres, a rough resin fracture, relatively clean fibres and more cusps than in any other mode.

Cusps in this particular resin system are very rare and considerable time is required with the SEM to locate them. In general, cusps are triangular shaped and oriented perpendicular to the crack propagation direction. This is in accordance with the results of

Table 2. The measured cusp angles for the different loading modes

Fracture mode	Measured cusp angle
Mixed mode 6:1	37.2°
Mixed mode 4:3	43.7°
Mixed mode 3:4	41.6°
Mixed mode 3:10	49.9°
Mode II	54.0°

Table 3. The density of fibre ends found for the different loading modes

Fracture mode	Density of fibre ends (mm ⁻²)
Mode I (static)	93.0
Mixed mode 6:1 (static)	17.3
Mixed mode 4:3 (static)	30.5
Mixed mode 3:4 (static)	4.4
Mixed mode 3:10 (static)	1.1
Mode II (static)	7.5
Mode I (fatigue)	54.8
Mixed mode 4:3 (fatigue)	3.7
Mode II (fatigue)	15.5

Smith and Grove,¹⁸ Carlsson *et al.*,¹⁰ and Purslow.⁴⁷ It was concluded that the use of stereo microscopy pairs is too tedious a method for determining the angle of inclination of cusps; instead, measurements at as high a tilt angle as possible are recommended. It is preferable that cusps from several locations on the surface should be used to average out any local variations in fracture mode that may be present as well as inevitable errors in the measurement of cusp angles. However, it is clear that pure mode II and mode II dominated mixed mode fractures can be relatively easily distinguished by the amount of cusps present on the fracture surface and also by the angle at which the cusps are oriented relative to the fracture surface.

The experimentally measured cusp angles are seen to increase with the component of mode II loading and this point is to be discussed in greater detail elsewhere. This is supported in similar work by Greenhalgh,⁴⁹ who reported an almost constant cusp angle for mode I dominated mixed modes which then increased rapidly for highly mode II dominated failures. From the observations of work of several authors^{7,13,15,16} and the results of the present investigation, it seems likely that the cusp angle can be used to determine the fracture mode with some confidence. Also, the cusp angles appear to be independent of the actual material system which supports the theory for microcrack formation. The determination of cusp angles must be simpler in a single phase matrix system where the cusps are more frequent and more clearly defined than in two phase resin systems such as 914 epoxy.

Several matrix features have shown a preference to form at the fibres of the underlying ply, as shown typically in Fig. 4. No similar observations have been found in the literature. This may be caused by failures very close to the boundary of the interlaminar resin region or by stress concentrations induced by the fibres. The phenomenon is probably dependent on the orientation of the fibres in the adjacent plies since a smoother fracture surface was seen at delaminations which did not occur along a cross-ply interface.⁴⁸ If

fracture propagated between two 0° plies, it would be assumed that this phenomenon would not be observed at all. The ply orientation also affects the general fracture surface. A cross-ply delamination has a rougher appearance than a unidirectional failure which was also observed by Smith and Grove.¹⁸ With regard to the different states of stress across the width of a specimen, no difference was found between cusps near the edge of a specimen and those along the midplane of a specimen. In a more brittle and single phase epoxy, where the cusps are numerous and well defined, it might be possible to detect such subtle differences (i.e. between plane stress and plane strain).

In some instances the orientation of the cusps along the edges of the non-adhesive inserts, used to simulate delamination, indicated that local fracture occurred from the edge insert and in towards the centre of the specimen, i.e. perpendicular to the main direction of delamination growth. The extent of such zones, however, was very small and this phenomenon was not commonly observed. Furthermore, some cusps were identified which indicated that the direction of delamination growth was coincident with the global crack direction; this is concluded to be the normal case. In any event, this only emphasises the importance of averaging the local directions of crack growth taken from many different locations in order that the global direction of damage propagation can be established with confidence.

In certain instances the opposing surfaces of a delamination can appear to be resin rich and resin starved. This occurs when fractures have taken place close to one ply boundary. In such cases, the resin features, mainly cusps, are almost solely found on the resin-rich mating surface. Both surfaces should therefore be examined in a fractographic analysis so that no vital information is missed.

Evidence has been found for the stress distribution proposed by Bascom *et al.*²⁴ around the fibres loaded in peel. Figure 7 shows resin flanges on a pulled-out fibre. In Fig. 6 minute cusps are seen (indicated by the arrows) as a result of the localised shear stresses present in the fibre/matrix separation process. This occurs around a fibre where the radial stress changes from tensile to compressive, causing local shear yielding to be induced in the matrix. This failure of the matrix material due to local shear yielding leaves flanges of resin on the edges of the fibres as they are peeled out.²⁴

The amount of fibre ends on the fracture surface was investigated for all modes since Friedrich¹⁹ had shown this to be significantly different for modes I and II. However, this characteristic was seen to be of only marginal importance. The general trend is that the fibre end density decreases rapidly from pure mode I to mode II dominated fractures. The different values

for static mixed mode I:II = 4:3 may be due to the fact that another specimen type was used for the testing (i.e. MMB versus ELS). The fatigue values for mode I and mixed mode 4:3 are significantly lower than the static values but for pure mode II the amount of broken fibres is twice that of a static failure. This is probably due to the different fibre fracture process in mode II. As the amount of fibre pull-out is dependent on specimen and material parameters^{8,19,50} this method of characterising different modes cannot be reliably used. From the results of the examination of this particular fibre/resin system, however, a very large number of broken fibres seems to be a characteristic of mode I failure.

A larger amount of resin debris and more PES nodules are present due to fatigue loading than in static failures; this was observed in all modes of loading and agrees with other workers.^{26,28,41} More nodules are present on the mode II surface than in mode I. Most of the resin features are worn down by the abrasion of the surfaces. This is also the reason for the cleaner fibres being observed, especially in mode II. Neither fatigue striations nor matrix rollers²⁸ could be found in any mode. That investigation utilised only unidirectional materials which may have had some influence on the formation of these features.

5 CONCLUSIONS

The present investigation has examined the fractographic features associated with delamination in multidirectional laminates of T300/914 carbon/epoxy composite. Delamination was constrained to occur along the $+45^\circ/-45^\circ$ interface of a $(-45^\circ/0^\circ/+45^\circ)_{2s}(+45^\circ/0^\circ/-45^\circ)_{2s}$ laminate by means of non-adhesive Kapton inserts. Pure mode I, pure mode II and mixed modes I/II of loading have been considered under both static and fatigue conditions. This entailed the use of DCB, ELS, FRMM and MMB fracture mechanics coupons. The 914 resin system proved difficult to investigate because of its two phase structure: this obscured most of the otherwise common resin features which made it especially difficult to determine the direction of crack propagation.

Cusps are generally very rare in all loading modes although the cusp angle was seen to increase with an increased mode II loading component from about 37° for mixed mode I:II = 6:1 to 54° for pure mode II. There are significantly more cusps in the mode II dominated fractures than in mode I fractures. The cusp angle is the most reliable method of determining the fracture mode. Fibre pull-out on its own can only be used to distinguish a highly mode I dominated surface. Further indications of a particular mode of fracture are acquired from ridge and valley markings and the overall surface appearance.

Fatigue failures on fracture specimens are distinguished by a generally worn appearance and the amount of resin debris and nodules that are present. More PES nodules are present on mode II fracture surfaces than in mode I. In structural components such as I-beams, however, failure will comprise of grinding and abrasion which will most likely result in more debris and nodules, even in static tests, than would be found in plane laboratory coupons such as the fracture mechanics specimens of the present investigation.

It is anticipated that future work in this area will concentrate on investigating the following:

- the effects of a varying stress state (plane stress and strain) across the width of a fracture specimen and the strain rate on the appearance and inclination of cusps, ideally in a single phase brittle resin, where features such as cusps can be studied in detail;
- the effects, if any, on resin features and pull-out with different types of fibres and coatings giving a different interfacial strength;
- the effect of environmental changes on the amount of cusps and the cusp angle.

ACKNOWLEDGEMENTS

This work was performed when the authors were at Imperial College, London, and they acknowledge Mr F. L. Matthews, of the Centre for Composite Materials, and Professors J. G. Williams and A. J. Kinloch, of the Mechanical Engineering Department, for their support throughout this time. The authors would like to thank Dr Stephen O. Osiyemi for providing the fracture toughness specimens for fractographic examination and Mr Emile Greenhalgh, of DRA Farnborough, for discussions concerning various fractographic features.

REFERENCES

1. Saliba, S. S. & Saliba, T. E., Computerization of fracture features and failure analysis of automotive composite materials. *Fractography of Modern Engineering Materials: Composites and Metals (Second Volume)*, ASTM STP 1203, ed. J. E. Masters & L. N. Gilbertson. American Society for Testing and Materials, Philadelphia, PA, 1994, pp. 23–57.
2. Wilkins, D. J., Eisenmann, J. S., Camin, R. A., Margolis, W. S. & Benson, R. A., Characterizing delamination growth in graphite-epoxy. *Damage in Composite Materials*, ASTM STP 775, ed. K. L. Reifsnider. American Society for Testing and Materials, Philadelphia, PA, 1982, pp. 168–83.
3. Williams, J. G., Fracture mechanics of composite failure, 26th John Player Lecture. *Proc. Institution of Mechanical Engineers*, 1990.
4. Hashemi, S., Kinloch, A. J. & Williams, J. G., The effects of geometry, rate and temperature on the mode I, mode II and mixed-mode I/II interlaminar fracture

- of carbon-fibre/poly(ether-ether ketone) composites. *J. Comp. Mater.*, **24** (1990) 918–56.
5. Reeder, J. D. & Crews Jr, J. H., Non-linear analysis and redesign of the mixed mode bending delamination test. NASA TM 102777, 1991.
6. Bradley, W. L., Relationship of matrix toughness to interlaminar fracture toughness. *Application of Fracture Mechanics to Composite Materials*, ed. K. Friedrich. Elsevier, Amsterdam, 1989, pp. 159–87.
7. Hibbs, M. F. & Bradley, W. L., Correlations between micromechanical failure processes and the delamination toughness of graphite/epoxy systems. *Fractography of Modern Engineering Materials: Composites and Metals*, ASTM STP 948, ed. J. E. Masters & J. J. Au. American Society for Testing and Materials, Philadelphia, PA, 1987, pp. 68–97.
8. Olsson, R., Factors influencing the interlaminar fracture toughness and its evaluation in composites. FFA Report FFA TN 1991-34, Stockholm, 1991.
9. Purslow, D., Matrix fractography of fibre-epoxy composites. Royal Aircraft Establishment, Technical Report 86046, 1986.
10. Carlsson, L. A., Trethewey, B. R. & Gillespie, J. W., Mode II cyclic delamination growth. *J. Comp. Mater.*, **22** (1988) 459–83.
11. Richards-Frandsen, R. & Naerheim, Y., Fracture morphology of graphite/epoxy composites. *J. Comp. Mater.*, **17** (1983) 105–13.
12. Donaldson, S. L., Fracture toughness testing of graphite/epoxy and graphite/PEEK composites. *Composites*, **16** (1985) 103–12.
13. Johannesson, T., Sjöblom, P. & Seldén, R., The detailed structure of delamination fracture surfaces in graphite/epoxy laminates. *J. Mater. Sci.*, **19** (1984) 1171–7.
14. Morris, G. E., Determining fracture directions and fracture origins on failed graphite/epoxy surfaces. *Nondestructive Evaluation and Flaw Criticality for Composite Materials*, ASTM STP 696, ed. R. B. Pipes. American Society for Testing and Materials, Philadelphia, PA, 1979, pp. 274–97.
15. Johannesson, T. & Blikstad, M., Fractography and fracture criteria of the delamination process, *Delamination and Debonding of Materials*, ASTM STP 876, ed. W. S. Johnson. American Society for Testing and Materials, Philadelphia, PA, 1985, pp. 411–23.
16. Arcan, L., Arcan, M. & Daniel, I. M., SEM fractography of pure and mixed-mode interlaminar fractures in graphite/epoxy composites. *Fractography of Modern Engineering Materials: Composites and Metals*, ASTM STP 948, ed. J. E. Masters & J. J. Au. American Society for Testing and Materials, Philadelphia, PA, 1987, pp. 41–67.
17. Lee, S. M., Fractography of composite materials. *International Encyclopedia of Composites*, Vol. 2. VCH Publishers, 1990, pp. 268–89.
18. Smith, B. W. & Grove, R. A., Determination of crack propagation directions in graphite/epoxy structures. *Fractography of Modern Engineering Materials: Composites and Metals*, ASTM STP 948, ed. J. E. Masters & J. J. Au. American Society for Testing and Materials, Philadelphia, PA, 1987, pp. 154–73.
19. Friedrich, K., Fractographic analysis of polymer composites. *Application of Fracture Mechanics to Composite Materials*, ed. K. Friedrich. Elsevier, Amsterdam, 1989, pp. 425–87.
20. Russell, A. J. & Street, K. N., The effect of matrix toughness on delamination: static and fatigue fracture

- under mode II shear loading of graphite fibre composites. *Toughened Composites*, ASTM STP 937, ed. N. J. Johnston. American Society for Testing and Materials, Philadelphia, 1987, pp. 275–94.
21. Donaldson, S. L., Mode III interlaminar fracture characterization of composite materials. *Comp. Sci. Technol.*, **32** (1988) 223–49.
 22. Robinson, P. & Song, D. Q., Development of a mode III delamination test for composites. *Proc. 2nd Int. Conf. on Deformation and Fracture of Composites*, Manchester, UK. Institute of Materials, 1993.
 23. Hahn, H. T. & Johannesson, T., A correlation between fracture energy and fracture morphology in mixed-mode fracture of composites. *Mechanical Behaviour of Materials IV, Proc. 4th Int. Conf.*, ed. J. Carlsson & N. G. Ohlsson. Pergamon Press, Oxford, 1984, pp. 431–8.
 24. Bascom, W. D., Boll, D. J., Fuller, B. & Phillips, P. J., Fractography of interlaminar fracture of carbon-fibre epoxy composites. *J. Mater. Sci.*, **20** (1985) 3184–90.
 25. Purslow, D., Fractographic analysis of failures in CFRP. *Characterisation, Analysis and Significance of Defects in Composite Materials*, AGARD, Conference Proceedings No 355M, London, 1983.
 26. Corberand, P. E. L., Micromechanisms of mode II fatigue delamination in continuous fibre polymer composites. MSc thesis, Cranfield Institute of Technology, Cranfield, UK, 1990.
 27. Marom, G., Environmental effects on fracture mechanical properties of polymer composites. *Application of Fracture Mechanics to Composite Materials*, ed. K. Friedrich. Elsevier, Amsterdam, 1989, pp. 397–424.
 28. Hiley, M. J. & Curtis, P. T., Mode II damage development in carbon fibre reinforced plastics. *AGARD: 74th Structures and Materials Meeting*, Patras, Greece, 1992.
 29. Franz, H. E., Characteristics of fatigue failures in fibre-reinforced plastics. Royal Aircraft Establishment, Library Translation 2081, 1992.
 30. Morris, G. E. & Hetter, C. M., Fractographic studies of graphite/epoxy fatigue specimens. *Damage in Composite Materials*, ASTM STP 775, ed. K. L. Reifsnider. American Society for Testing and Materials, Philadelphia, PA, 1982, pp. 27–39.
 31. Scrivner, G. C. & Chan, W. S., Effects of stress ratio on edge delamination characteristics in laminated composites. *Composite Materials: Fatigue and Fracture (Fourth Volume)*, ASTM STP 1156, ed. W. W. Stinchomb & N. E. Ashbough. American Society for Testing and Materials, Philadelphia, PA, 1993, pp. 538–51.
 32. deRenzo, D. J., *Advanced Composite Materials: Products and Manufacturers*. Noyes Data Corporation, 1988.
 33. Watts, J. F., Cazeneuve, C. & Castle, J. E., The structure of the interface in carbon fibre composites by scanning auger microscopy. *J. Mater. Sci.*, **25** (1990) 1902–8.
 34. Partridge, I. K., High temperature thermosetting matrix resins. *Advanced Composites*, ed. I. K. Partridge. Elsevier, 1989, pp. 7–41.
 35. Yamanaka, K. & Inoue, T., Structure development in epoxy resin modified with poly(ether sulphone). *Polymer*, **30** (1989) 663–7.
 36. Lowe, A., Structure and matrix dominated properties of T300/914 carbon epoxy composites. PhD thesis, Department of Material Science and Metallurgy, Cambridge University, 1992.
 37. Bucknall, C. B. & Partridge, I. K., Phase separation in epoxy resins containing polyethersulphone. *Polymer*, **24** (1983) 639–44.
 38. Bucknall, C. B. & Partridge, I. K., Effects of morphology in the epoxy/PES matrix on the fatigue behaviour of uniaxial CFRP. *Composites*, **15** (1984) 129–33.
 39. Davies, P., The effect of temperature on the interlaminar fracture of tough composites. *Proc. 6th Int. Conf. on Composite Materials (ICCM-VI)*, Vol 3. Elsevier, London, 1987, pp. 3284–94.
 40. deCharentenay, F. X., Harry, J. M., Prel, Y. J. & Benzeggagh, M. L., Characterizing the effect of delamination defect by mode I delamination test. *Effects of Defects in Composite Materials*, ASTM STP 836, ed. J. R. Schroeder. American Society for Testing and Materials, Philadelphia, PA, 1984, pp. 84–103.
 41. Henaff-Gardin, C. & Lafarie-Frenot, M. C., Fatigue behaviour of thermoset and thermoplastic cross-ply laminates. *Composites*, **23** (1992) 109–16.
 42. Sawyer, L. C. & Grubb, D. T., *Polymer Microscopy*. Chapman & Hall, 1987.
 43. Shikhmanter, L., Cina, B. & Eldror, I., Fractography of multidirectional CFRP composites tested statically. *Composites*, **22** (1991) 437–44.
 44. Russell, A. J. & Street, K. N., Factors affecting the interlaminar fracture energy of graphite/epoxy laminates. *Progress in Science and Engineering of Composites, 4th Int. Conf. on Composite Materials (ICCM-IV)*, Tokyo, 1982, pp. 279–86.
 45. Marom, G., Roman, I., Harel, H., Rosensaft, M., Kenig, S. & Moshonov, M., The characterization of mode I and mode II delamination failures in fabric-reinforced laminates. *Proc. 6th Int. Conf. on Composite Materials (ICCM-VI)*, Vol 3. Elsevier, London, 1987, pp. 3265–73.
 46. Purslow, D., Further fractographic characteristics of peel failure in CFRP. *Composites*, **18** (1987) 255–6.
 47. Purslow, D., Some fundamental aspects of composite fractography. Royal Aircraft Establishment, Technical Report 81127, 1981.
 48. Svensson, N., A fractographic analysis of the failure of multidirectional carbon/epoxy T300/914 laminates. MSc dissertation, Centre for Composite Materials, Imperial College, London, 1994.
 49. Greenhalgh, E. S., Defence Research Agency, private communication, 1994.
 50. Hu, X. Z. & Mai, Y. W., Mode I delamination and fibre bridging in carbon-fibre/epoxy composites with and without PVAL coating. *Comp. Sci. Technol.*, **46** (1993) 147–56.